Acta Mechanica 44, 201—222 (1982)

ACTA MECHANICA

The Influence of Biaxiality of Loading on the Form of Caustics in Cracked Plates

By

P. S. Theocaris and **G. A. Papadopoulos**, Athens, Greece

With 13 Figures

(*Received June 1, 1981*)

Summary

The optical method of reflected caustics was applied up-to-now to problems of cracked plates under uniaxial loading. Only the problem of the biaxial tension of the plate has been considered for the particular case where the crack is transverse to the longitudinal axis of the plate which coincided with the loading axis. In this paper the influence of a biaxial loading of the plate on the form and orientation of the caustic was studied in connection with the orientation of the crack. New modified relations were given for the evaluation of the complex stress intensity factor $K = K_I - iK_{II}$ in terms of the angle φ of the angular displacement of the caustic axis. For the accurate evaluation of K_I and K_{II} nomograms of correction factors $\delta_{y'}^{\max}$, $\delta_{x'}^{\max}$ and $\delta_{x'}^{\min}$ were given in terms of the angle of inclination of the crack $\omega = (90 - \beta)$ and the biaxiality factor k. Experimental evidence with PMMA internally cracked plates corroborated the results of theory.

List of Symbols

$\Phi(z)$, $\Omega(z)$	complex-stress function of Muskhelishvili
σ_{xx}, σ_{yy}, τ_{xy}	crack tip stress referred to Cartesian coordinate system
r, ϑ	polar coordinate system centered at crack tip
K_I, K_{II}	stress intensity factors for Mode I and II loading, respectively
ω	angle of inclination of the crack
β	90°-ω
k	ratio of stresses at infinity
σ_1, σ_2	principal stresses at crack tip
a	crack length
σ	stress applied at infinity along the transverse boundaries of the plate
$X'_{r,f}$, $Y'_{r,f}$	parametric equations of the reflected caustics referred to the Cartesian system $O'X'Y'$ on the reference screen: (r) reflected caustics from rear face of the specimen and (f) reflected caustics from the front face of the specimen
r_0	radius of the generatrix curve on the specimen around the crack tip (initial curve)
$c_{r,f}$	optical constants of the material for reflections from the rear and front faces of the specimen respectively
Λ_m	magnification ratio of the optical set-up
z_0	distance between the reference-screen and the middle plane of the specimen
z_i	distance between the focus of the light beam and the middle plane of the specimen

0001-5970/82/0044/0201/$04.40

d	thickness of specimen
ε	2 for the reflected caustics from the rear face of the specimen and 1 for the reflected caustics from the front face of the specimen
$C_{r,f}$	$\varepsilon z_0 dc_{r,f}/\lambda_m(2\pi)^{1/2}$
ν	Poisson's ratio
E	elastic modulus of the material
A	$(1+k)+(1-k)\cos 2\omega$
B	$(1-k)\sin 2\omega$
C	$1+k^2+(1-k^2)\cos 2\omega$
φ	$2\tan^{-1}(B/A) = 2\tan^{-1}(K_{II}/K_I)$
$D_{y'}^{\max}$, $D_{x'}^{\max}$, $D_{x'}^{\min}$	the maximum and the minimum diameter of caustics along the axis $O'y'$ and $O'x'$ of the crack respectively
$\delta_{y'}^{\max}$, $\delta_{x'}^{\max}$, $\delta_{x'}^{\min}$	the correction factors for $D_{y'}^{\max}$, $D_{x'}^{\max}$ and $D_{x'}^{\min}$ respectively
$D_t^{\max}$, $D_l^{\max}$	the maximum transverse and longitudinal diameters of the caustics respectively
$\delta_t^{\max}$, $\delta_l^{\max}$	the correction factors for $D_t^{\max}$ and $D_l^{\max}$ respectively

1. Introduction

The optical method of reflected caustics, as it has been developed during the last ten years, was extensively applied to various elastic problems containing singularities and especially to problems with cracked plates. Whereas in all these problems of cracked plates under any combination of the three modes of deformation were studied, in the case of uniaxial loading of the plate, the problem of the influence of the biaxiality of loading was strangely always omitted. Surely, it was taken into account the influence of the component of stress parallel to the crack tip which was added to the singular expression of stresses, but this was valid only for the case when the crack-axis was normal to the applied tensile load at infinity.

It was only in 1977 that Liebowitz and his co-workers [1] to [4] have considered problems of infinite plates containing slant cracks where the influence of biaxiality of loading of the plate was taken into account for stationary cracks. Thus, Eftis, Subramonian and Liebowitz [1] have shown that the one-parameter representation of the stress field at the vicinity of the crack tip only for simple cases of transverse cracks and uniaxial normal to the crack-axis loadings is a satisfactory approximation. When a biaxial load at infinity is applied to the cracked plate and the crack is oblique to the principal applied stresses to the plate this representation may lead to erroneous results. It was also shown that the second term in the series representation for the stresses contributes significantly and independently of the distance from the crack tip. The effect of higher terms was best indicated in the problem of a biaxially loaded infinite plate containing a transverse central crack [2] under biaxial loading at infinity. Liebowitz and co-workers continued their study on the influence of biaxiality and have shown in a third paper [3] that the elastic strain energy density depends also on the biaxiality of the applied load. Finally, in a fourth paper Liebowitz, Lee and Eftis [4] have shown that the elastic stress intensity factor as well as the j-integral are not sensitive to the presence of the biaxial load. They extended also their studies to internal cracks in finite plates and to cases small scale yielding.

Simultaneously, some extensive experimental studies with photoelasticity were undertaken where crack-tip stress patterns were analysed on the basis of two and multiple parameter characterization of the stress components at the vicinity of the

crack tip. It was shown that at least a two-parameter representation of the stress field around the crack tip is necessary and in many cases sufficient to yield results in agreement with the experiment [5] to [9]. For a critical review of these two-parameter methods see ref. [9].

A three-parameter method taking into account the third term in the Taylor series expansion of the Westergaard complex stress function was introduced in ref. [10] for the evaluation of mode-I stress intensity factor at a crack tip where the idea of an appropriate selection of the polar direction for determining K_I was introduced depending on the distance of the point of measurement of isochromatics from the crack tip. Three and several terms approximations in the series expansions of $Z(z)$ were also introduced in refs. [11] and [12] in order to liberate the measurements from the requirement of being made at the vicinity of the crack tip, but these methods are rather complicated and necessitate considerable computer work with doubtful results. Finally, Rossmanith gave an extensive analysis of the mixed-mode isochromatic patterns at the vicinity of the crack tip in a plate containing an oblique crack [13].

On the other hand, Cotterell [14] studied the influence that the coefficient of the second term of the Williams asymptotic expansion has on the shape and orientation of the isostatic loops. Similarly, Williams and Ewing [15] have studied the influence of the applied biaxial stress at infinity in a plate containing an internal slant crack and discussed the influence of the constant term in the Taylor series expansion of the stress function on the position of the critical angle of fracture. The procedure adopted in the experiments indicates empirically the significance of inclusion of the constant and higher terms of the series expansion of the Westergaard complex stress function. However fails to disclose the authentic influence of these terms on the stress distribution around the crack tip and consequently on the form of the isochromatics.

With caustics the situation is different. While the isochromatics are proportional to $|\bar{z}\Phi'(z) + \Psi(z)|$ (where $\Phi(z)$ and $\Psi(z) = -2\Phi(z)/z$ the Muskhelishvili complex stress functions) and the isopachics are proportional to Re $\Phi(z)$ in caustics the initial curve and the respective caustic depend on $\Phi''(z)$ and $\overline{\Phi'(z)}$ respectively and at least for the K_I-mode of deformation of the crack these curves are independent of the constant term, at least, in the series expansion of $\Phi(z)$. An extensive study of the influence of the biaxiality factor k on the dynamic crack propagation in slant cracks of any obliqueness was undertaken by Theocaris [16] and Theocaris and Papadopoulos [17], whereas closed-form solutions for the stress field in cracked plates under biaxial load was recently prepared [18].

In this paper the influence of biaxiality on the shape and orientation of caustics formed around stationary cracks was thoroughly studied and formulas were given for evaluating K_I and K_{II} for any slant angle β of the crack where this influence is incorporated by the introduction of appropriate correction factors.

2. Crack-Tip Stress Fields for Mixed-Mode Deformation

For a thin elastic and isotropic plate under conditions of generalized plane stress containing a slant internal crack of length $2a$ and submitted at infinity by a biaxial state of stress defined by the stresses σ and $k\sigma$ along two adjacent sides

of the plate (Fig. 1) the Muskhelishvili complex stress functions $\Phi(z)$ and $\Omega(z)$ are given by [19]

$$\Phi(z) = \frac{1}{2}(2\Gamma + \bar{\Gamma}')\frac{z}{(z^2 - a^2)^{1/2}} - \frac{1}{2}\bar{\Gamma}' \tag{1}$$

and

$$\Omega(z) = \frac{1}{2}(2\Gamma + \bar{\Gamma}')\frac{z}{(z^2 - a^2)^{1/2}} + \frac{1}{2}\bar{\Gamma}' \tag{2}$$

where the quantities Γ and $\bar{\Gamma}'$ are expressed by:

$$\frac{1}{2}\bar{\Gamma}' = -\frac{\sigma}{4}(1 - k)\, e^{2i\left(\frac{\pi}{2} - \omega\right)} \tag{3}$$

$$\frac{1}{2}(2\Gamma + \bar{\Gamma}') = \frac{\sigma}{4}\left\{\left[1 - e^{2i\left(\frac{\pi}{2} - \omega\right)}\right] + k\left[1 + e^{2i\left(\frac{\pi}{2} - \omega\right)}\right]\right\}. \tag{4}$$

In these relations k is the biaxiality factor of the stresses at infinity and ω the angle subtended by the crack-axis and the transverse axis of the specimen ($\omega = 90° - \beta$). The components of stresses at the tip of the crack may be derived by the well-known relations:

$$\sigma_{xx} + \sigma_{yy} = 2[\Phi(z) + \overline{\Phi(z)}] \tag{5}$$

$$\sigma_{yy} - \sigma_{xx} + 2i\tau_{xy} = 2[(\bar{z} - z)\,\Phi'(z) + \bar{\Omega}(z) - \Phi(z)]. \tag{6}$$

Introducing relations (1) and (2) into relations (5) and (6) we obtain [1] to [3]:

$$\sigma_{xx} \cong \frac{K_I}{\sqrt{2\pi r}}\cos\frac{\vartheta}{2}\left[1 - \sin\frac{\vartheta}{2}\sin\frac{3\vartheta}{2}\right] - \frac{K_{II}}{\sqrt{2\pi r}}\sin\frac{\vartheta}{2}\left[2 + \cos\frac{\vartheta}{2}\cos\frac{3\vartheta}{2}\right] - \sigma(1 - k)\cos 2\omega \tag{7}$$

$$\sigma_{yy} \cong \frac{K_I}{\sqrt{2\pi r}}\cos\frac{\vartheta}{2}\left[1 + \sin\frac{\vartheta}{2}\sin\frac{3\vartheta}{2}\right] + \frac{K_{II}}{\sqrt{2\pi r}}\sin\frac{\vartheta}{2}\cos\frac{\vartheta}{2}\cos\frac{3\vartheta}{2} \tag{8}$$

$$\tau_{xy} \cong \frac{K_I}{\sqrt{2\pi r}}\sin\frac{\vartheta}{2}\cos\frac{\vartheta}{2}\cos\frac{3\vartheta}{2} + \frac{K_{II}}{\sqrt{2\pi r}}\cos\frac{\vartheta}{2}\left[1 - \sin\frac{\vartheta}{2}\sin\frac{3\vartheta}{2}\right] \tag{9}$$

where the components of the stress intensity factor $K = K_I - iK_{II}$ are given by:

$$K_I = \frac{\sigma\sqrt{\pi a}}{2}\cdot A \tag{10}$$

$$K_{II} = \frac{\sigma\sqrt{\pi a}}{2}\cdot B \tag{11}$$

with:

$$A = (1 + k) + (1 - k)\cos 2\omega \tag{12}$$

$$B = (1 - k)\sin 2\omega. \tag{13}$$

The variation of the K_I- and K_{II}-stress intensity factors in terms either of the angle ω of inclination of the crack-axis with the transverse direction or of the

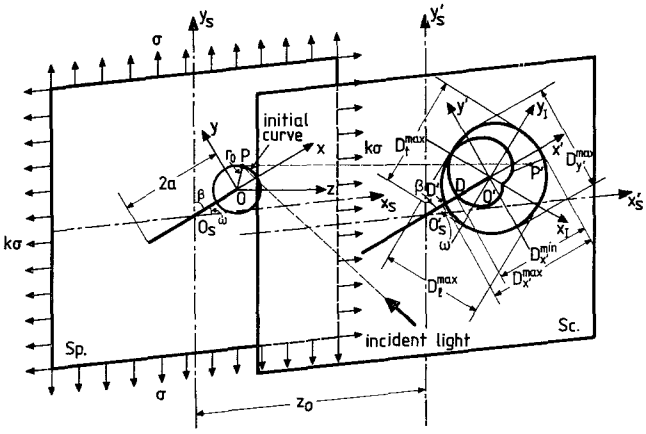

Fig. 1. Geometry of cracked plate and the shape of the principal epicycloid and geometry of its formation for $k = 0$ (uniaxial tension)

biaxiality factor k is given in Fig. 2 and 3 respectively. Similarly, the variation of ratio of stress intensity factors K_{II}/K_I versus ω and k is given in Figs 4(a, b) respectively. From relations (7) and (8) the sum of principal stresses at the vicinity of the crack tip may be evaluated from relation:

$$(\sigma_1 + \sigma_2) = (\sigma_{xx} + \sigma_{yy}) = \frac{2}{(2\pi r)^{1/2}} \left(K_I \cos \frac{\vartheta}{2} - K_{II} \sin \frac{\vartheta}{2} \right) - \sigma(1 - k) \cos 2\omega. \tag{14}$$

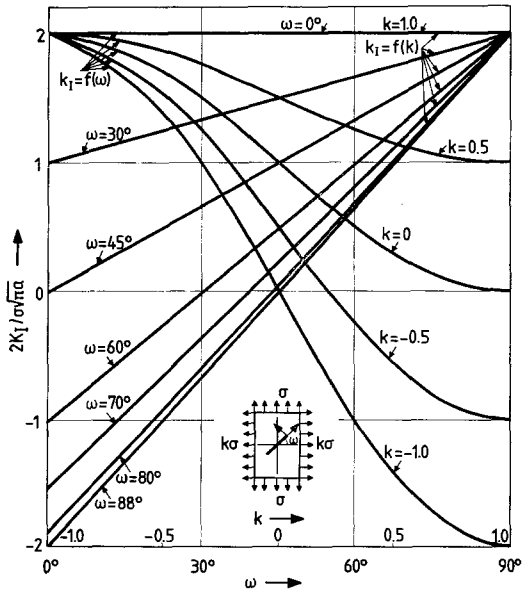

Fig. 2. Variation of K_I versus either ω, or k for various parametric values of k and ω respectively

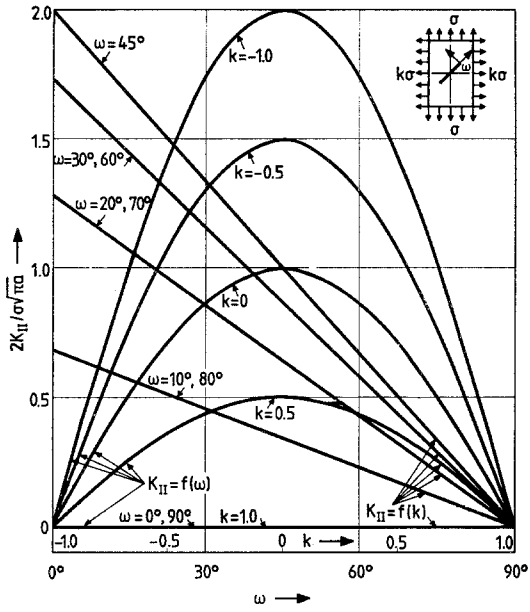

Fig. 3. Variation of K_{II} versus either ω, or k for various parametric values of k and ω respectively

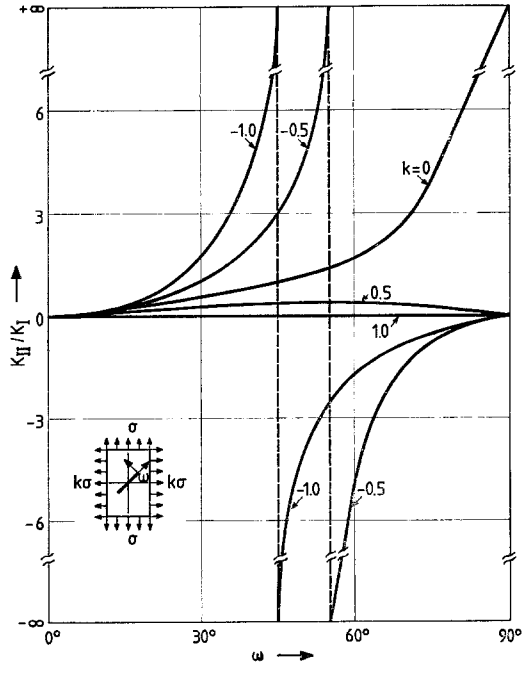

Fig. 4a. Variation of the ratio K_{II}/K_I versus ω for various parametric values of k

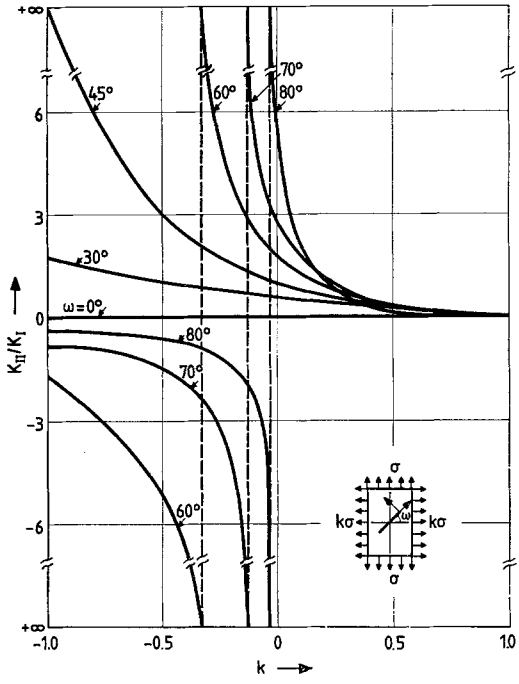

Fig. 4b. Variation of the ratio K_{II}/K_I versus k for various parametric values of ω

3. The Method of Reflected Caustics for Biaxial Loading

The experimental arrangement of the method is simple. A laser light, the specimen, a ground glass screen and a camera suffice for recording the caustics. It is shown schematically in Fig. 1 while at both lateral faces of the specimen the generatrix curves of the respective caustics are small circles, on the screen *Sc* the external caustic corresponds to reflections from the rear and the internal caustic to reflections from the front face of the specimen.

It has been shown that for uniaxial tension (or compression) with $k = 0$ the parametric equations for both branches of the caustic are given by [20]:

$$\lambda_m^{-1} x'_{r,f} = r_0 \cos\vartheta + C_{r,f} K_I r_0^{-3/2} \cos\frac{3\vartheta}{2} - C_{r,f} K_{II} r_0^{-3/2} \sin\frac{3\vartheta}{2} \tag{15}$$

$$\lambda_m^{-1} y'_{r,f} = r_0 \sin\vartheta + C_{r,f} K_I r_0^{-3/2} \sin\frac{3\vartheta}{2} + C_{r,f} K_{II} r_0^{-3/2} \cos\frac{3\vartheta}{2} \tag{16}$$

where r_0 expresses the radius of the generatrix curve (initial curve) given by:

$$r_0 = \left(\frac{3}{2} C_{r,f}\right)^{2/5} (K_I^2 + K_{II}^2)^{1/5} \tag{17}$$

with:

$$C_{r,f} = \frac{\varepsilon z_0 \, dc_{r,f}}{\lambda_m (2\pi)^{1/2}}. \tag{18}$$

In relation (18) the quantity ε takes either the value $\varepsilon = 2$ for reflected rays from the rear face of the cracked plates (caustics designated with the subscript r), or the value $\varepsilon = 1$ for reflected from the front face rays, d is the thickness of the plate and $C_{r,f}$ global constants including the optical constants of the material as well as it mechanical properties and corresponding to reflected rays from the rear (r) or the front face (f) of the plate. The constant c_f is very simple and equals:

$$c_f = \nu/E, \tag{19}$$

where ν is Poisson's ratio and E the elastic modulus of the material. Finally, the magnification ratio of the optical set-up λ_m is given by:

$$\lambda_m = \frac{z_0 \pm z_i}{z_i} \tag{20}$$

where z_i is the distance between the focus of the light source and the middle plane of the plate and z_0 the distance between this plane and the parallel plane of the reference screen Sc. The positive sign is valid for real image, while the negative one for virtual image.

Introducing relations (10) and (11) into Eq. (17) we obtain:

$$r_0 = \left(\frac{3}{2} C_{r,f} \sigma \sqrt{\pi a}\right)^{2/5} \left(\frac{C}{2}\right)^{1/5} \tag{21}$$

with:

$$C = 1 + k^2 + (1 - k^2) \cos 2\omega. \tag{22}$$

Relation (21) yields the depedence of the radius r_0 of the initial curve from the angle ω and the biaxiality factor k. The complete variation of the radius r_0 of the initial curve versus either the angle ω, or the biaxiality factor k with parameter the other quantity for each case is given in Fig. 5.

Introducing relation (21) into Eqs. (15) and (16) we obtain the parametric equations of the caustic in terms of ω and k. These relations are given by:

$$\lambda_m^{-1} x'_{r,f} = r_0 \left\{\cos\vartheta + \frac{2}{3} A(2C)^{-1/2} \cos\frac{3\vartheta}{2} - \frac{2}{3} B(2C)^{-1/2} \sin\frac{3\vartheta}{2}\right\} \tag{23}$$

$$\lambda_m^{-1} y'_{r,f} = r_0 \left\{\sin\vartheta + \frac{2}{3} A(2C)^{-1/2} \sin\frac{3\vartheta}{2} + \frac{2}{3} B(2C)^{-1/2} \cos\frac{3\vartheta}{2}\right\}. \tag{24}$$

Relations (23) and (24) are the parametric equations of the caustic referred to the $0'x'y'$-system (Fig. 1). By angularly displacing the $0'x'y'$-system by an angle $(2\pi - \varphi)$ we obtain the new $0'x_Iy_I$-system. For this new coordinate system relations (23) and (24) may be found by the transformation:

$$\begin{pmatrix} x_{I_{r,f}} \\ y_{I_{r,f}} \end{pmatrix} = \begin{pmatrix} \cos\varphi & -\sin\varphi \\ \sin\varphi & \cos\varphi \end{pmatrix} \begin{pmatrix} x'_{r,f} \\ y'_{r,f} \end{pmatrix}. \tag{25}$$

These relations in the new coordinate system become:

$$x_{I_{r,f}} = \lambda_m r_0 \left\{\cos(\vartheta + \varphi) + \frac{2}{3} \cos\left(\frac{3\vartheta}{2} + \gamma + \varphi\right)\right\} \tag{26}$$

$$y_{I_{r,f}} = \lambda_m r_0 \left\{\sin(\vartheta + \varphi) + \frac{2}{3} \sin\left(\frac{3\vartheta}{2} + \gamma + \varphi\right)\right\} \tag{27}$$

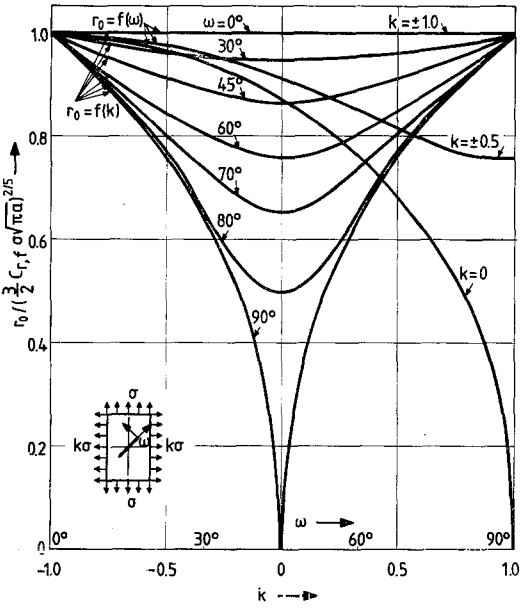

Fig. 5. Variation of the radius r_0 of the initial curve versus either ω, or k for various parametric values of k and ω respectively

with

$$\cos\gamma = A(2C)^{-1/2}, \tag{28}$$

$$\sin\gamma = B(2C)^{-1/2} \tag{29}$$

and

$$\sin^2\gamma + \cos^2\gamma = 1. \tag{30}$$

Putting $\gamma = \varphi/2$ and $\tau = (\vartheta + \varphi)$ the parametric Eqs. (26) and (27) become:

$$x_{I_{r,f}} = \lambda_m r_0 \left\{\cos\tau + \frac{2}{3}\cos\frac{3\tau}{2}\right\} \tag{31}$$

$$y_{I_{r,f}} = \lambda_m r_0 \left\{\sin\tau + \frac{2}{3}\sin\frac{3\tau}{2}\right\}. \tag{32}$$

It may be derived from the parametric Eqs. (31) and (32) that the caustic in the $0'x_Iy_I$-reference system is a symmetric curve having as an axis of symmetry the line subtending an angle $-\varphi$ with the $0'x'$-axis of the crack. Relations (28) and (29) for $\gamma = \varphi/2$ yield the angle of angular displacement of the caustic relatively to the crack-axis. This angle is given by:

$$\varphi = 2\tan^{-1}\frac{(1-k)\sin 2\omega}{(1+k)+(1-k)\cos 2\omega}. \tag{33}$$

Comparing relation (33) with relations (10) and (11) we obtain:

$$\varphi = 2\tan^{-1}\frac{K_{II}}{K_I}. \tag{34}$$

Therefore, relations (33) and (34) yield the angle of angular displacement of the caustic in terms of the angle ω of inclination of the crack and the biaxiality factor k. The variation of angle φ with angle ω and the factor k is given in Figs. 6a, b.

From relations (23) and (24), for values of ϑ between $-\pi$ and π and for various values of the biaxiality factor k we may readily plot the caustics formed around the respective crack tips.

For $k = 1$ the caustics plotted are always symmetric to the crack axis while for $k \neq 1$ and varying beteeen $k = -1$ and $k = 1$ a continuous relative rotation

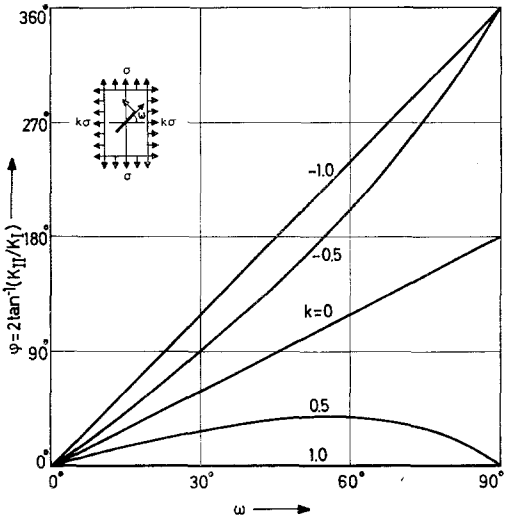

Fig. 6a. Variation of the angle φ of rotation of caustic versus ω for various parametric values of k

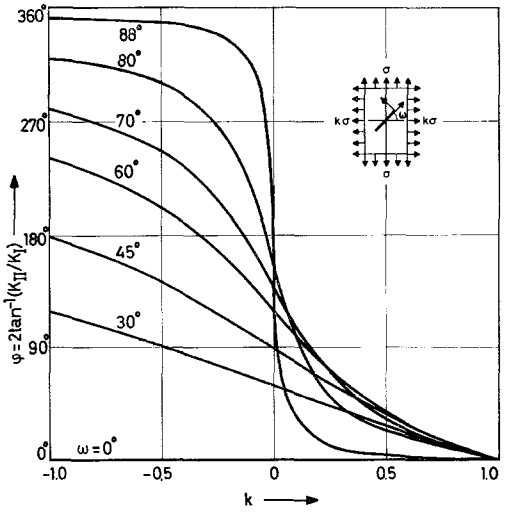

Fig. 6b. Variation of the angle φ of rotation of caustic versus k for various parametric values of ω

of the caustic is apparent. This rotation is made in such a direction so that the crack axis and the axis of symmetry of the caustic subtend an angle equal to $-\varphi$ given by relations (33) and (34).

Figs. 7a, b present a series of caustics plotted by the computer for typical

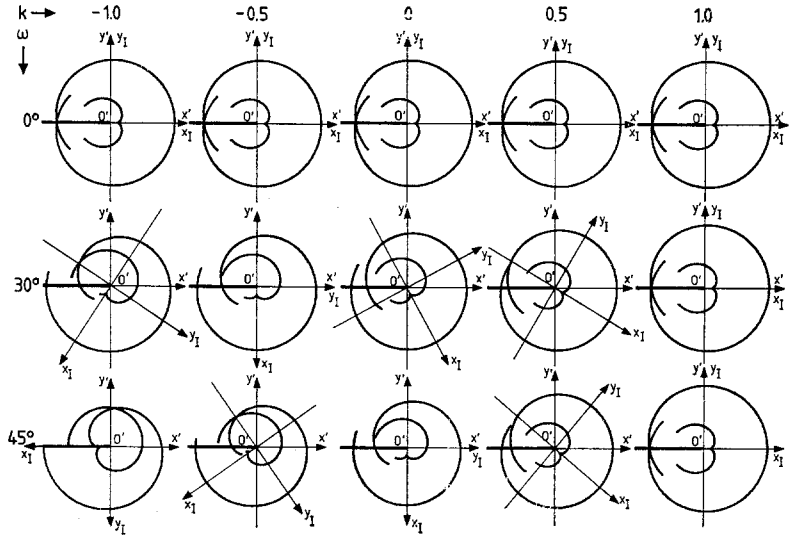

Fig. 7a. The caustics from reflected light rays on a cracked plate made of an isotropic elastic material for k between -1 and 1 and for $\omega = 0°$, 30° and 45° as they have been plotted by the computer for $-\pi \leqq \vartheta \leqq \pi$

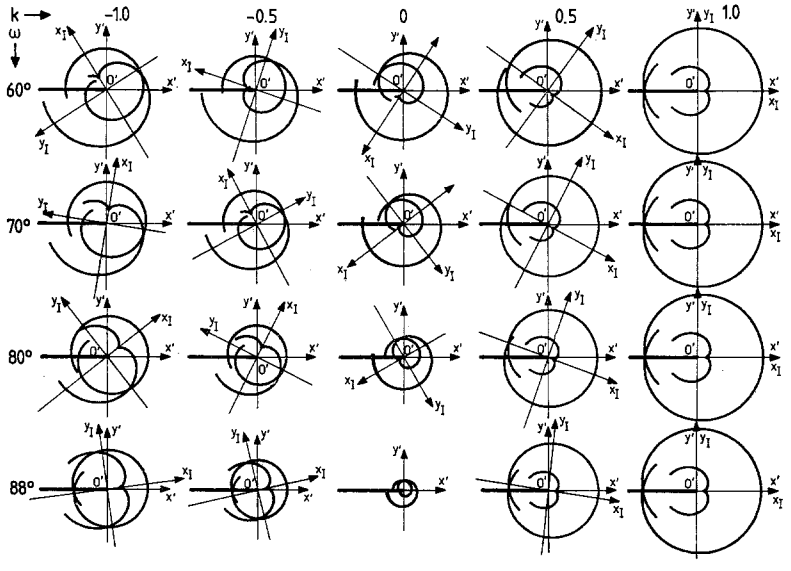

Fig. 7b. The caustics from reflected light rays on a cracked plate made of an isotropic elastic material for k between -1 and 1 and for $\omega = 60°$, 70°, 80° and 88° as they have been plotted by the computer for $-\pi \leqq \vartheta \leqq \pi$

values of angle ω ($\omega = 0°, 30°, 45°, 60°, 70°, 80°$ and $88°$) and values of k varying between $k = -1$ and $k = 1$. These caustics correspond to an initially isotropic and elastic material and as such was chosen PMMA with $\nu = 0.34$ and $E = 3400$ MN/m^2. The thickness of the cracked plate was $d = 0.003$ m the crack length $2a = 0.02$ m and the optical constant $c_r = -1.55 \times 10^{-10}$ m^2/N, $z_0 = 2.0$ m, $z_i = 0.5$ m and $\sigma = 2.0$ MN/m^2.

4. Evaluation of the Diameters $D_{t,l}^{\max}$ of the Caustics and the Stress Intensity Factors K_I and K_{II}

Relation (24) presents extrema whose positions may be found by zeroing the first derivative $\partial y'_{r,f}/\partial\vartheta$. This derivation yields:

$$\lambda_m^{-1}\,\partial y'_{r,f}/\partial\vartheta = r_0\left\{\cos\vartheta + A(2C)^{-1/2}\cos\frac{3\vartheta}{2} - B(2C)^{-1/2}\sin\frac{3\vartheta}{2}\right\} = 0 \quad (35)$$

with:

$$r_0 = \left(\frac{3}{2}\,C_{r,f}K_I\right)^{2/5}\left(1 + \frac{B^2}{A^2}\right)^{1/5}. \quad (36)$$

Solutions of relation (35) for $-1 \leqq k \leqq 1$ and for $0° \leqq \omega < 90°$ yield the positions of angles $\vartheta_{y',j}^{\max}$ for which the maxima of relation (21) exist (these are maxima since $\partial^2 y'_{r,f}/\partial\vartheta^2 < 0$). Relation (24) may be written under the form:

$$D_{y'}^{\max} = \sum_{j=1}^{2} y_{r,f,j}^{\max} = \lambda_m\left(\frac{3}{2}\,C_{r,f}K_I\right)^{2/5}\delta_{y'}^{\max}(\omega, k), \quad (37)$$

where $D_{y'}^{\max}$ expresses the maximum diameter of the caustic along the direction of the $0'y'$-axis of the crack and $\delta_{y'}^{\max}(\omega, k)$ is a correction factor given by:

$$\delta_{y'}^{\max}(\omega, k) = \sum_{j=1}^{2}\left(1 + \frac{B^2}{A^2}\right)^{1/5} \cdot\left\{\sin\vartheta_{y',j}^{\max} + \frac{2}{3}\,A(2C)^{-1/2}\sin\frac{3\vartheta_{y',j}^{\max}}{2} + \frac{2}{3}\,B(2C)^{-1/2}\cos\frac{3\vartheta_{y',j}^{\max}}{2}\right\}. \quad (38)$$

The maximum and minimum values $D_{x'}^{\max}$, $D_{x'}^{\min}$ of the diameter of the caustic along the $0'x'$-axis of the crack may be evaluated from relation (23) for values of angles $\vartheta_{x'}^{\max}$ and $\vartheta_{x'}^{\min}$ for which relation (24) becomes equal to zero. For these values relation (23) may be put under the form:

$$D_{x'}^{\max,\min} = \sum_{j=1}^{2} x_{r,f,j}^{\max,\min} = \lambda_m\left(\frac{3}{2}\,C_{r,f}K_I\right)^{2/5}\delta_{x'}^{\max,\min}(\omega, k), \quad (39)$$

where again $D_{x'}^{\max}$ and $D_{x'}^{\min}$ are the maximum and minimum diameters of the caustic along the $0'x'$-axis of the crack and $\delta_{x'}^{\max}(\omega, k)$ and $\delta_{x'}^{\min}(\omega, k)$ the respective

correction factors given by:

$$\delta_{x'}^{\max,\min}(\omega, k) = \sum_{j=1}^{2} \left(1 + \frac{B^2}{A^2}\right)^{1/5} \cdot \left[\cos \vartheta_{x',j}^{\max,\min} + \frac{2}{3} A(2C)^{-1/2} \cos \frac{3\vartheta_{x',j}^{\max,\min}}{2} - \frac{2}{3} B(2C)^{-1/2} \sin \frac{3\vartheta_{x',j}^{\max,\min}}{2}\right]. \tag{40}$$

The variations of the correction factors $\delta_{y'}^{\max}$, $\delta_{x'}^{\max}$ and $\delta_{x'}^{\min}$ in terms of the angle ω and the factor k are given in Figs. 8a, b, 9a, b and 10a, b respectively.

From relation (39) we may derive the ratio $(D_{x'}^{\max} - D_{x'}^{\min})/D_{x'}^{\max}$ given by:

$$\frac{D_{x'}^{\max} - D_{x'}^{\min}}{D_{x'}^{\max}} = \frac{\delta_{x'}^{\max} - \delta_{x'}^{\min}}{\delta_{x'}^{\max}}. \tag{41}$$

From this relation it may be derived that the difference of the respective maximum $(D_{x'}^{\max})$ and minimum $(D_{x'}^{\min})$ diameters of the caustic along the $0'x'$-axis of the crack normalized to $D_{x'}^{\max}$ equals the respective difference of the correction factors $\delta_{x'}^{\max}$ and $\delta_{x'}^{\min}$ normalized to $\delta_{x'}^{\max}$.

The variation of the ratio (41) in terms of the angle ω and the factor k is given in Figs. 11a, b.

Finally, from relations (18), (34), (37) and (39) the stress intensity factors K_I and K_{II} may be evaluated from the respective relations:

$$K_I = \pm \frac{2(2\pi)^{1/2}}{3\varepsilon z_0 \, d\lambda_m^{3/2} |\, c_{r,f}|} \left(\frac{D_{y'}^{\max}}{\delta_{y'}^{\max}}\right)^{5/2} \tag{42}$$

or:

$$K_I = \pm \frac{2(2\pi)^{1/2}}{3\varepsilon z_0 \, d\lambda_m^{3/2} |\, c_{r,f}|} \left(\frac{D_{x'}^{\max,\min}}{\delta_{x'}^{\max,\min}}\right) \tag{43}$$

and:

$$K_{II} = K_I \tan \frac{\varphi}{2}. \tag{44}$$

Relations (42), (43) and (44) yield the components of stress intensity factors derived by measuring the diameters $D_{y'}^{\max}$ and $D_{x'}^{\max,\min}$ of the caustics along the transverse and the longitudinal axes of the crack. The sign of K_I must be chosen according to Fig. 2. However, since the internal caustic yields always the $0'x_I$-axis of symmetry of both caustics an alternative procedure, which is, in some cases, much easier than the previous one, is to measure the diameters $D_t^{\max}$ and $D_l^{\max}$ of the caustic. These diameters are along $0'y_I$- and $0'x_I$-axes which may be defined by tracing the common tangent to the cuspoid internal caustic and draw the normal at the middle of this common tangent. This normal is the $0'x_I$-axis of the caustic. In this case the two components K_I and K_{II} are expressed by:

$$K_I = \pm \frac{2(2\pi)^{1/2}}{3\varepsilon z_0 \, d\lambda_m^{3/2} |c_{r,f}|} \left(\frac{D_{t,l}^{\max}}{\delta_{t,l}^{\max}}\right)^{5/2} \tag{45}$$

$$K_{II} = K_I \tan \frac{\varphi}{2}. \tag{46}$$

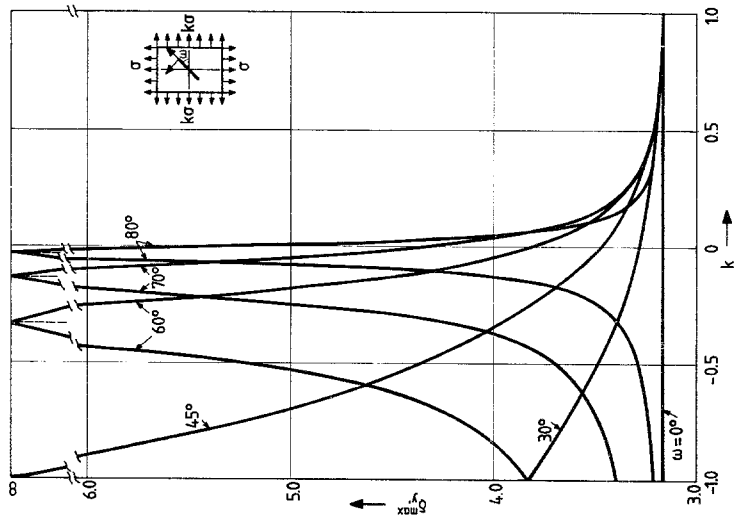

Fig. 8b. Variation of the correction factor $\delta_{y'}^{\max}$ versus k for various parametric values of ω

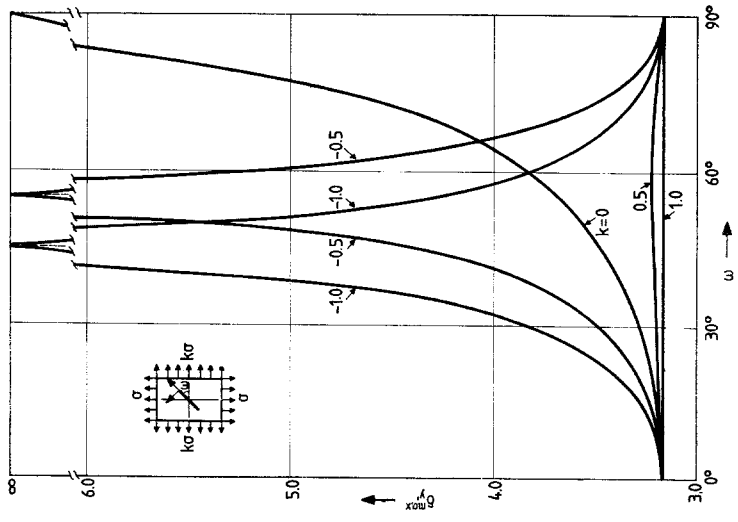

Fig. 8a. Variation of the correction factor $\delta_{y'}^{\max}$ versus ω for various parametric values of k

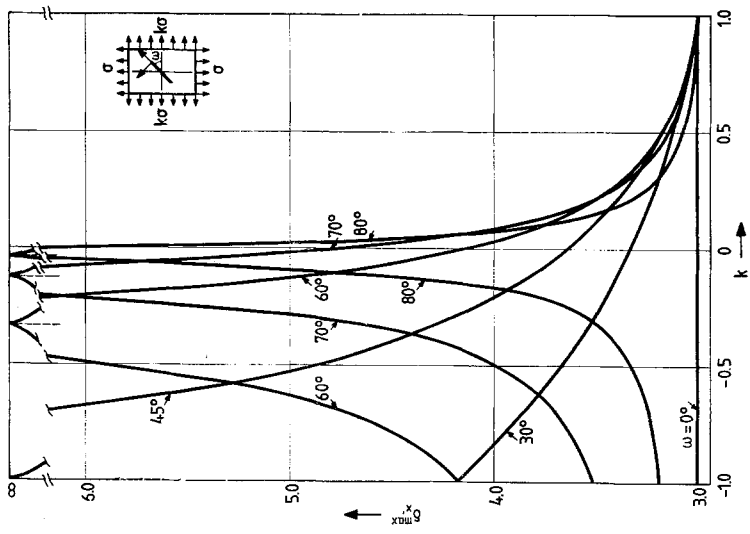

Fig. 9b. Variation of the correction factor $\delta_{x'}^{max}$ versus k for various parametric values of ω

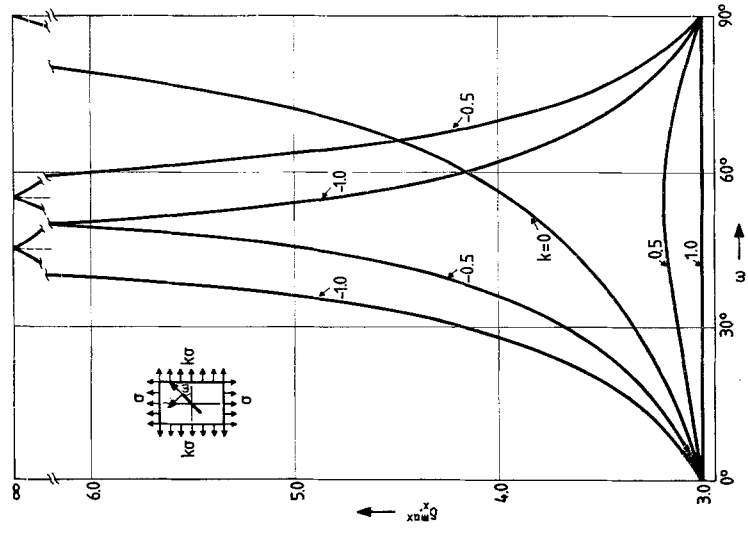

Fig. 9a. Variation of the correction factor $\delta_{x'}^{max}$ versus ω for various parametric values of k

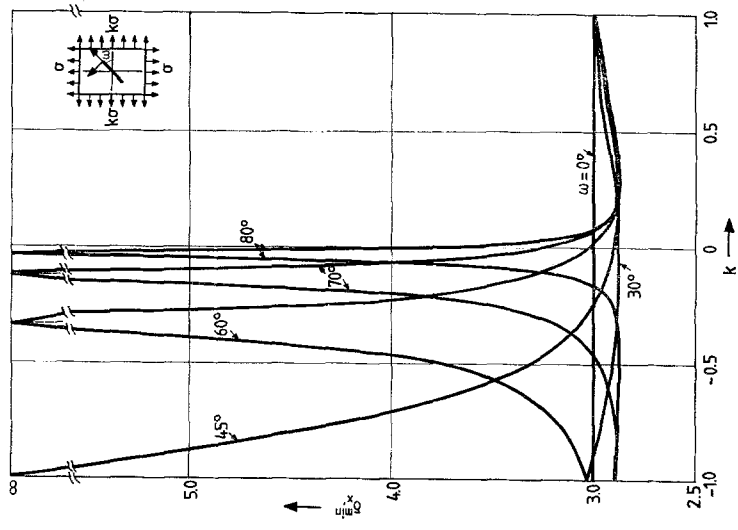

Fig. 10b. Variation of the correction factor $\delta_{x'}^{\min}$ versus k for various parametric values of ω

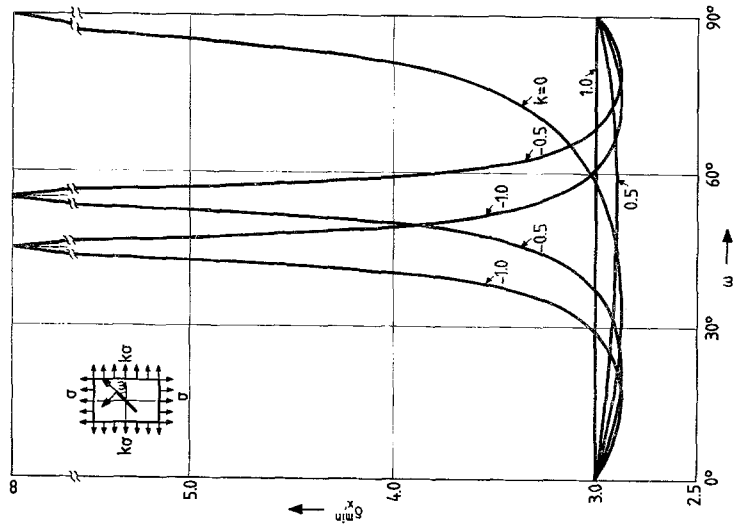

Fig. 10a. Variation of the correction factor $\delta_{x'}^{\min}$ versus ω for various parametric values of k

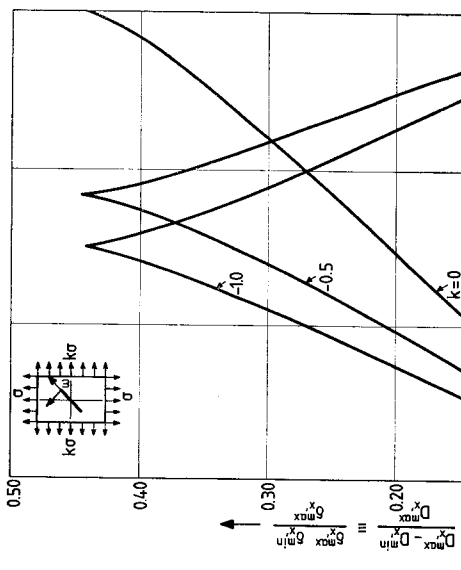

Fig. 11a. Variation of the ratio $(D_{x'}^{max} - D_{x'}^{min})/D_{x'}^{max}$ of the maximum and minimum longitudinal diameters of the caustics versus ω for various parametric values of k

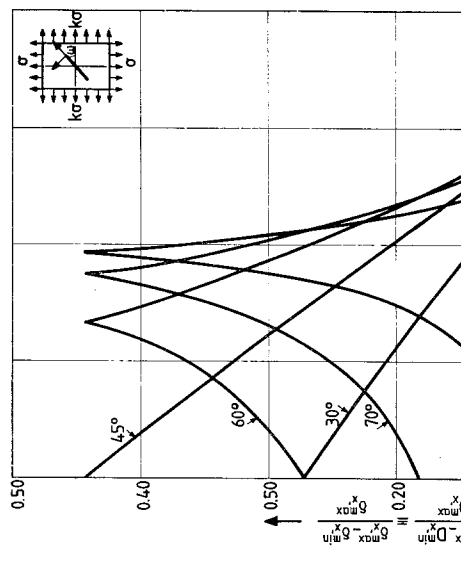

Fig. 11b. Variation of the ratio $(D_{x'}^{max} - D_{x'}^{min})/D_{x'}^{max}$ of the maximum and minimum longitudinal diameters of the caustics versus k for various parametric values of ω

In relations (45) the correction factors $\delta_t^{\max}$ and $\delta_l^{\max}$ take the values $\delta_t^{\max} = 3.17$ and $\delta_l^{\max} = 3.00$ respectively. These well known values may be derived from the nomograms of Figs. 8a, b, 9a, b and 10a, b for $\omega = 0°$ or $k = 1.0$.

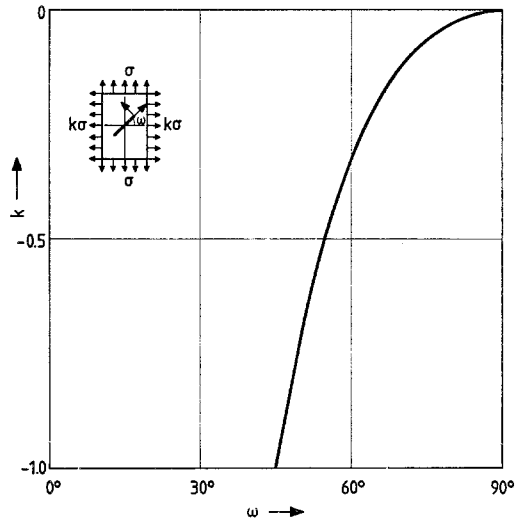

Fig. 12. Positions where appears the state of stress in the vicinity of the crack tip is pure shear ($K_I = 0$, $K_{II} \neq 0$) for $k < 0$, while for $k > 0$ there are no positions of pure shear

5. Experimental Evidence

In order to check the potentialities of the method we have applied it for the evaluation of the angle φ of the angular displacement of the caustic in a thin plate containing a central crack subtending an angle $\omega = 45°$ to the loading axis and subjected to a biaxial load at infinity. The material of the plate was plexiglas with $\nu = 0.34$, $E = 3400\,\mathrm{MN/m^2}$ and an optical constant $c_r = -1.55 \times 10^{-10}\,\mathrm{m^2/N}$. The specimens had the following average dimensions: width $w = 0.15$ m, thickness $d = 0.003$ m, and crack length $2a = 0.02$ m.

Fig. 13 presents the experimentally obtained caustics formed on a reference screen placed at a distance $z_0 = 2.0$ m from the specimen, for four cases of biaxial load with $\sigma = 1.5\,\mathrm{MN/m^2}$. Fig. 13a presents the reflected caustic with a biaxiality factor $k = -1.0$ (equal tension-compression). The angle of angular displacement of the caustic is $\varphi = 180°$ while Fig. 13b presents the reflected caustic with $k = -0.6$ (tension-compression) and the angle $\varphi = 150°$, Fig. 13c shows the reflected caustic for the case where $k = 0.7$ (tension-tension) and the angle $\varphi = 20°$. Finally, Fig. 13d presents the reflected caustic with $k = 1.0$ (equal tension-tension) and the angle $\varphi = 0°$. All the experimentally measured angles φ coincide with the theoretically obtained ones derived from Figs. 6a and b.

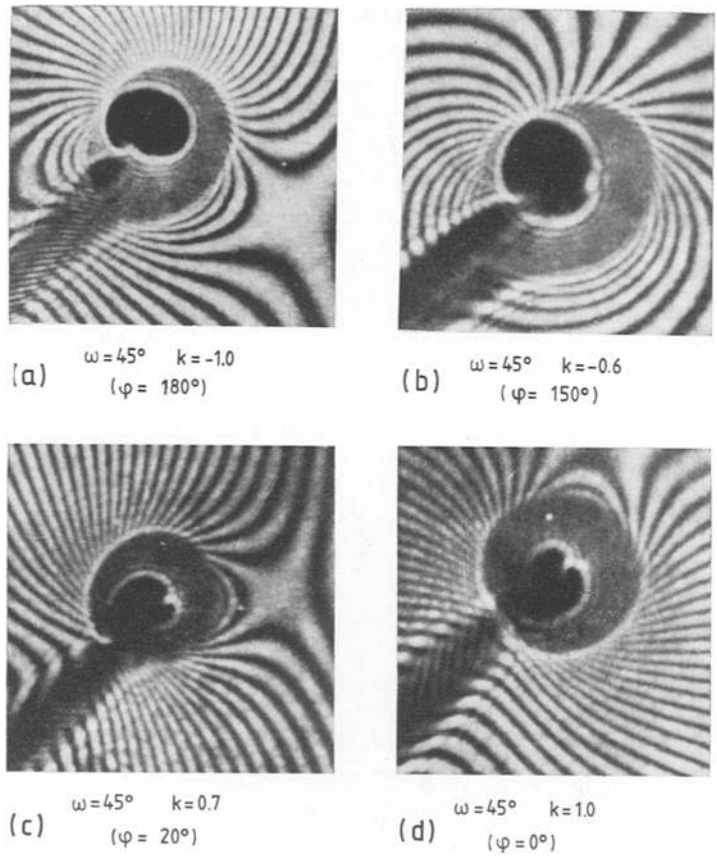

Fig. 13. Experimentally obtained reflected caustics for plexiglas plate containing a central crack with angle of inclination $\omega = 45°$ and subjected to biaxial load with $\sigma = 1.5$ MN/m² and for k (a) —1.0 (b) —0.6 (c) 0.7 and (d) 1.0

6. Results and Discussion

In this paper a method was developed for evaluating the components of the stress intensity factor $K = K_I - iK_{II}$ by measuring on the reflected caustics created around the crack tip of a slant crack existing in an infinite elastic plate submitted to any type of in-plane biaxial loading.

The influence of the angle of inclination of the crack ω ($\omega = 90° - \beta$), as well as of the biaxiality factor k expressing the ratio of loading of the plate at infinity is apparent by following the variation of the shape and orientation of the respective caustics for each case with ω and k. Figs. 7a, b exemplify this influence.

The influence of the angle ω and the factor k on the values of K_I and K_{II} appears in Figs. 2 and 3. It may be derived from these figures that as the angle ω increases and therefore angle β decreases there is also a decrease of K_I. The same phenomenon happens for decreasing values of k. On the contrary, the values for

K_{II} increase from zero for $\omega = 0°$ rapidly to a maximum appearing for $\omega \cong 45°$ followed by a decrease of this factor which becomes again zero for $\beta = 0°$ ($\omega = 90°$).

The values of K_I-factor for positive values of the biaxiality factor k tend from a positive value maximum value which appears at $\beta = 90°$ ($\omega = 0°$) to zero, whereas for negative values of k this factor takes negative values. In the positions where a change of sign for K_I appears the state of stress in the vicinity of the crack tip is pure shear ($K_I = 0$, $K_{II} \neq 0$). In these positions of pure shear the ratio K_{II}/K_I tends to infinity fact appearing in Figs. 4a, b.

The shape and the size of caustics depend on the values of the radius of the initial curve as it is clear from relations (23) and (24). The inclination of the crack axis ω and the biaxiality of the external loading k influence the size of the initial curve as this appears in Figs. 5. For increasing values of ω and for $k < 0$, a decrease of the magnitude of the radius r_0 of the initial curve appears which after passing from a minimum value corresponding to $k = 0$ it starts to increase continuously for $k > 0$. For $\omega = 0°$ the size of the initial curve remains constant and independent of k.

The same phenomenon happens for $k = \pm 1$ for any angle of inclination ω. While this is valid for the size of the initial curves, for the respective caustics these are independent of ω and k only for $k = 1$ and $\omega = 0°$. For values of $k = -1$ the size of the caustics and their orientation depend on ω. This may be explained by the fact that while for $k = 1$ the state of stress of the plate at infinity is biaxial tension, that is a symmetric case, for $k = -1$ the state of stress becomes longitudinal tension and transverse compression, which influences weakly the size of the caustics but strongly their orientation. Indeed, as it may be seen from Figs. 7a, b the cusp of the internal caustic has been angularly displaced by $-\pi$ for ω varying between zero and 45°. For ω varying between zero and $\pi/2$ the cusp is angularly displaced by -2π. On the other hand the external branch of the caustic is continuously reduced in size while its extremities alternate on both sides of the crack.

In Figs. 6a, b, where the dependence of the angle of angular displacement of the caustic in terms of angle ω and the factor k is given, it is indicated that for $k \geqq 0$ the axis of symmetry of the respective caustic coincides with the crack-axis for $\omega = 0°$ and it is angularly displaced by an angle $-\varphi$ for different values of ω. This angle $-\varphi$ is progressively decreasing as ω increases for $k \leq 0$.

The dependence of angle φ on k is as follows: For $k = 1$ angle φ is independent of ω and β. For positive values of k its variation presents a smooth maximum. For $k = 0$ the dependence of φ on ω is linear and for $\omega = 90°$ angle φ takes the value $\varphi = 180°$. For k positive angle φ takes always positive values.

In the position of pure shear $K_I = 0$ and $K_{II} \neq 0$, an interchange appears of the branches of the caustics that is the external almost circular branch becomes internal and the internal cuspoid branch becomes external. The measurements of diameter for evaluating K_I and K_{II} should be made on this external branch which corresponds to rays reflected from the front face of the plate and therefore for the evaluation of K's the optical constant c_f should now be taken into consideration instead of c_r.

Similar phenomena appear with the variation of φ in terms of k. For values of $\omega = 0°$, φ is independent of k as it was expected from previous evidence [16].

From the nomograms of Figs. 8 to 10 we observe that the values of the correction factors $\delta_{y'}^{\max}$, $\delta_{x'}^{\max}$ and $\delta_{x'}^{\min}$ are increasing with increasing values of ω and k and after passing through infinity they diminish tending to their asymptotic values corresponding to $\omega = 0°$ that is $\delta_t^{\max} = 3.1702$ and $\delta_l^{\max} = 3.00$. The positions of infinite values for the correction factors correspond to pure shear stress fields around the cracks and the positions of jump for the angle φ as it was previously discussed.

Finally, Figs. 11a, b yield the variation of the distance DD' of the intersections of the external branch of the caustic with the crack lips with ω and k respectively. It is observed that at the positions of pure shear at the crack tip the maximum of such distance between the fails of the caustic appears. A combination of Figs. 6a, b and 11a, b leads to the evaluation of the angle of rotation of the caustic and therefore to an evaluation of K_{II} especially in cases where the angle φ of rotation of the caustic is difficult to be evaluated especially in cases where the method is applied to opaque materials.

Finally, in Fig. 12 the positions where the stress distributions at the crack tip is pure shear, with $K_I = 0$ and $K_{II} \neq 0$, are shown. It must be said that this stress distribution can only be achieved when $k < 0$, while for $k > 0$ such positions do not exist.

References

[1] Eftis, J., Subramonian, N., Liebowitz, H.: Crack border stress and displacement equations revisited. Engrg. Fract. Mech. **9**, 189 (1977).

[2] Eftis, J., Subramonian, N.: The inclined crack under biaxial load. Engrg. Fract. Mech. **10**, 43 (1978).

[3] Eftis, J., Subramonian, N., Liebowitz, H.: Biaxial load effects on the crack border elastic strain energy and strain energy rate. Engrg. Fract. Mech. **9**, 753 (1977).

[4] Liebowitz, H., Lee, J. D., Eftis, J.: Biaxial load effects in fracture mechanics. Engrg. Fract. Mech. **10**, 315 (1978).

[5] Irwin, G. R.: Discussion on: The dynamic stress distribution surrounding a running crack — A photoelastic analysis. Proc. Soc. Exp. Stress Analysis **16**, 93 (1958).

[6] Smith, D. G., Smith, C. W.: Photoelastic determination of mixed mode stress intensity factors. Engrg. Fract. Mech. **4**, 357 (1972).

[7] Theocaris, P. S., Gdoutos, E.: A photoelastic determination of K_I stress intensity factors. Engrg. Fract. Mech. **7**, 331 (1975).

[8] Theocaris, P. S., Gdoutos, E. E.: Discussion on: Limitations of the Westergaard equation for experimental evaluations of stress intensity factors [by W. T. Evans and A. R. Luxmoore, J. Strain Analysis **11**, 177 (1976)]. J. Strain Analysis **12**, 349 (1977).

[9] Etheridge, J. M., Dally, J. W.: A critical review of methods for determining stress-intensity factors from isochromatic fringes. Exp. Mech. **17**, 248 (1977).

[10] Ioakimides, N., Theocaris, P. S.: A simple method for the photoelastic determination of mode I stress intensity factors. Engrg. Fract. Mech. **10**, 677 (1978).

[11] Sanford, R. J., Dally, J. W.: A general method for determining mixed-mode stress intensity factors from isochromatic fringe patterns. Engrg. Fract. Mech. **11**, 621 (1979).

[12] Dally, J. W., Sanford, R. J.: Classification of stress-intensity factors from isochromatic-fringe patterns. Exp. Mech. **18**, 441 (1978).

[13] Rossmanith, H. P.: Analysis of mixed mode isochromatic crack-tip fringe patterns. Acta Mechanica **34**, 1 (1979).

[14] Cotterell, B.: Notes on the paths and stability of cracks. Int. J. Fract. Mech. **2**, 526 (1966).

[15] Williams, J. G., Ewing, P. D.: Fracture under complex stress-angled crack problem. Int. J. Fract. Mech. 8, 441 (1972).
[16] Theocaris, P. S.: The elastic strain-energy density in cracked plates derived from caustics. Proc. Intern. Symposium on absorbed specific energy and strain energy density criterion, in Memory of Late Professor L. Gillemot, Budapest, 1980 (Sih, G., Czoboly, E., Gillemot, eds.), pp. 17—39. M. Nijhoff. 1981.
[17] Theocaris, P. S., Papadopoulos, G.: Mixed-mode elastodynamic forms of caustics for running cracks under constant velocity. Proc. U.S.-Greece symposium on mixed mode crack propagation (Sih, G. C., Theocaris, P. S., eds.), p. 125. Sijthoff and Noordhoff. 1981.
[18] Theocaris, P. S., Michopoulos, J.: The exact from of caustics in mixed-mode fracture. A comparison with approximate solutions. (To be published.)
[19] Muskhelishvili, N. I.: Some basic problems of the mathematical theory of elasticity, 4th ed. Groningen: Noordhoff 1963.
[20] Theocaris, P. S., Gdoutos, E. E.: An optical method for determining opening-mode and edge sliding-mode stress-intensity factors. J. Appl. Mech. **39**, 91 (1972).

Prof. P. S. Theocaris and G. A. Papadopoulos
Department of Theoretical and Applied Mechanics
The National Technical University of Athens
5, K. Zographou Street
Zographou, Athens 624, Greece